ELSEVIER

Colloids and Surfaces
A: Physicochemical and Engineering Aspects 187–188 (2001) 509–521

COLLOIDS AND SURFACES A

www.elsevier.nl/locate/colsurfa

# Relaxation of polymers in 2 nm slit-pores: confinement induced segmental dynamics and suppression of the glass transition

E. Manias [a,*], V. Kuppa [a], D.-K. Yang [b], D.B. Zax [b]

[a] *Materials Science and Engineering department, The Pennsylvania State University, 325-D Steidle Building, University Park, PA 16802, USA*

[b] *Department of Chemistry and Chemical Biology, Cornell University, Ithaca, NY, USA*

**Abstract**

Molecular Dynamics (MD) simulations are used to explore the structure and dynamics of polystyrene confined in 2 nm slit pores, between parallel, crystalline, mica-type surfaces. The systems simulated resemble experimentally studied intercalated nanocomposites, where polystyrene is inserted between layered-silicate layers. The molecular modeling perspective complements the experimental findings and provides insight into the nature of polymers in nanoscopic confinements, especially into the molecular origins of their macroscopic behavior. Namely, a comparison between simulation and NMR studies shows a coexistence of extremely faster and much slower segmental motions than the ones found in the corresponding bulk polymer at the same temperature. The origins of these dynamical inhomogeneities are traced to the confinement induced density modulations inside the 2 nm slits. Fast relaxing phenyl and backbone moieties are found in low density regions across the film, and preferentially in the center, whereas slow relaxing moieties are concentrated in denser regions in the immediate vicinity of the confining surfaces. At the same time, the temperature dependence of the segmental relaxations suggests that the glass transition is suppressed inside the confined films, an observation confirmed by scanning calorimetry. 

*Keywords:* Dynamics; Glass transition; Calorimetry

## 1. Introduction

Polymers and simple fluids in nanoscopic confinements possess a variety of unusual properties, and in particular remarkable dynamical heterogeneities which vary on length scales as short as a few Angstroms [1–13]. While the Surface Forces Apparatus (SFA) provides an experimental probe of macroscopic properties of a single fluid film between two atomically-smooth mica surfaces [14–16], few experimental probes are available which probe the microscopic origins of these heterogeneities in nanoscopically confined films. However, ultra-thin ($\sim$2–5 nm) polymer films

* Corresponding author. Tel.: +1-814-8632980; fax: +1-814-8652917.

*E-mail address:* manias@psu.edu (E. Manias).

0927-7757/01/$ - see front matter 
PII: S0927-7757(01)00634-3

confined between solid surfaces can be created by intercalating high molecular weight polymers in between allumino-phyllosilicates (mica-type layered crystals). Especially where appropriately modified silicates are used to form intercalated nanocomposites very homogeneous ultra-thin confined polymer structures self-assemble throughout the composite [17,18]. In such cases, careful choice of the polymer/inorganic stoichiometry can provide macroscopic quantities of self-assembled multilayer systems, which consist exclusively of identical nanoconfined films. This offers great opportunity to study the properties of polymers and liquids in extreme confinements (1–2 nm) by employing conventional analytical techniques [17].

For this reason, intercalated polymer/mica-type silicate nanocomposites have been recently investigated with the emphasis on the fundamentals of nanoscopically confined polymers [19,20]. It has been found that the nanoscopic confinement between solid surfaces affects the polymer behavior in ways that are not intuitively expected. Additionally, in many cases this confinement-modified polymeric structure and dynamics have been shown to dictate the materials response at the macroscopic level [17], causing remarkable enhancements of the materials properties [18].

Here, we report a molecular modeling approach, combined with NMR experimental findings, aiming in obtaining insight into the confinement induced dynamical processes of ultra-thin polystyrene films in 2 nm slit pores. Studying the formation, structure and dynamics of these intercalated structures can lead to a better understanding of polymers in a confined environment or at a solid interface, and at the same time provide the necessary fundamental level knowledge towards the molecular design of polymer/inorganic hybrid materials with desirable properties.

## 2. Simulation model and details

Inspired by striking new experimental findings of polymer films in 2 nm slit pores between alkylammonium modified mica-type surfaces [19,20], we performed extensive Molecular Dynamics (MD) computer simulations of polystyrene (PS) in 2 nm slits. Following we will mention some of the essential details of the simulations, more in [21].

The simulation geometry resembles closely the systems studied by NMR [20]. Our simulation boxes are $4.224 \times 3.656 \times 3.05$ and $2.112 \times 1.828 \times 3.05$ nm in dimensions, with periodic boundary conditions in all three directions (Fig. 1). A solid surface with the crystal structure of a synthetic 2:1 mica-type silicate is placed parallel to the $xy$ plane, thus confining the organic molecules in the $z$ direction. The confinement size (3.05 nm) was selected to correspond to the experimentally measured X-ray diffraction d-spacing

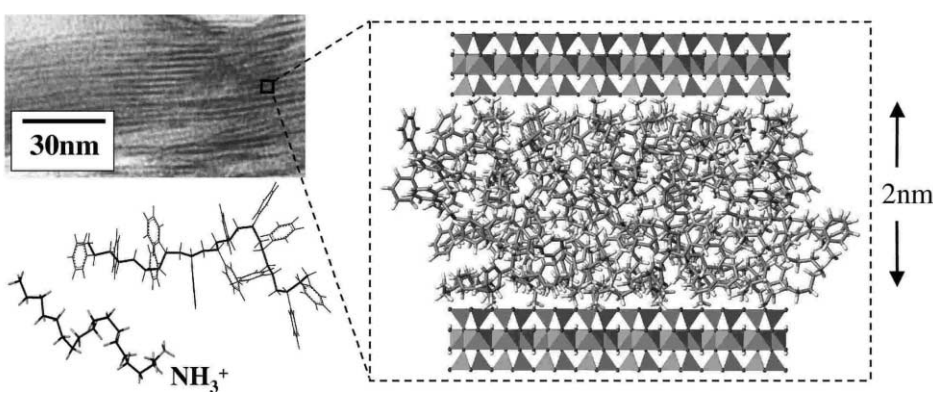


Fig. 1. The system under investigation. From top left clockwise: a bright-field TEM detail of the PS/octadecyl-ammonium silicate intercalate; a snapshot of the simulation box; a styrene 12 monomers (the smaller of the two PS molecules simulated) and the octadecyl-ammonium surfactant molecule.

Table 1
The force-field parameters used in the MD simulations; bonded and non-bonded interactions are given for the organic species in the systems

| | | | |
|---|---|---|---|
| Non-bonded interactions | $V(r_{ij}) = 4\varepsilon\,[(\sigma/r_{ij})^{12} - (\sigma/r_{ij})^{6}] + (1/4\pi\varepsilon)q_i q_j/r_{ij}$ | | |
| | $\sigma$ (nm) | $\varepsilon$ (kJ mol$^{-1}$) | q (e) |
| C | 0.3207 | 0.3519 | 0.000 |
| $C_{ph}$ | 0.3550 | 0.2940 | 0.115 |
| $C_{ph}$[a] | 0.3550 | 0.2940 | 0.000 |
| H | 0.2318 | 0.3182 | 0.000 |
| $H_{ph}$ | 0.2420 | 0.1260 | −0.115 |
| N | 0.2976 | 0.8767 | 0.000 |
| Bond-stretching potentials | $V(r) = (k_b/2)(r - b_o)^2$ | | |
| | $b_o$ (nm) | $k_b$ (kJ mol$^{-1}$) | |
| C–C | 0.153 | 334720 | |
| $C_{ph}$–C | 0.151 | 418400 | |
| $C_{ph}$–$C_{ph}$ | 0.139 | 418400 | |
| C–N | 0.133 | 376560 | |
| C–H | 0.109 | 292880 | |
| $C_{ph}$–H | 0.108 | 292880 | |
| N–H | 0.100 | 374468 | |
| Bond-angle potentials | $V(\theta) = (k_\theta/2)(\theta_{ijh} - \theta_o)^2$ | | |
| | $\theta_o$ (°) | $k_\theta$ (kJ per (mol rad$^2$)) | |
| H–C–H | 109.45 | 306.40 | |
| C–C–H | 109.45 | 366.90 | |
| $C_{ph}$–C–H | 109.45 | 366.90 | |
| C–C–C | 109.45 | 482.30 | |
| C–C–$C_{ph}$ | 109.45 | 482.30 | |
| C–$C_{ph}$–$C_{ph}$ | 120.00 | 376.60 | |
| $C_{ph}$–$C_{ph}$–$C_{ph}$ | 120.00 | 376.60 | |
| $C_{ph}$–$C_{ph}$–H | 120.00 | 418.80 | |
| H–N–H | 109.45 | 306.40 | |
| N–C–H | 109.45 | 366.90 | |
| C–C–N | 109.45 | 482.30 | |
| Proper dihedrals | $V_{ijkl}(\phi) = k_\phi[1 + \cos(n\phi - \phi_o)]$, cis at 0° and $\phi \equiv (ijk) \angle (jkl)$ | | |
| | $\phi_o$ (°) | $k_\phi$ (kJ mol$^{-1}$) | $N$ |
| C–C–C–C | 0.0 | 5.88 | 3 |
| C–C–C–N | 0.0 | 5.88 | 3 |
| C–C–C–H[b] | 0.0 | 5.88 | 3 |
| C–C–N–H[b] | 0.0 | 5.88 | 3 |
| Planar (improper) | $V_{ijkl}(\xi) = k_\xi(\xi - \xi_o)^2$, $i$ central $C_{ph}$ and $\xi \equiv (ijk) \angle (jkl)$ | | |
| | $\xi$ (°) | $k_\xi$ (kJ mol$^{-1}$) | |
| $C_{ph}$–$C_{ph}$–$C_{ph}$–$C_{ph}$ | 0.0 | 167.36 | |
| $C'_{ph}$–$C_{ph}$–$C_{ph}$–$H_{ph}$ (on $i$) | 0.0 | 167.36 | |
| $C'_{ph}$–$C_{ph}$–$C_{ph}$–C (on $i$) | 0.0 | 167.36 | |

[a] The phenyl carbon connected to the backbone methine.
[b] The hydrogens of the chain-end methyls and ammoniums.

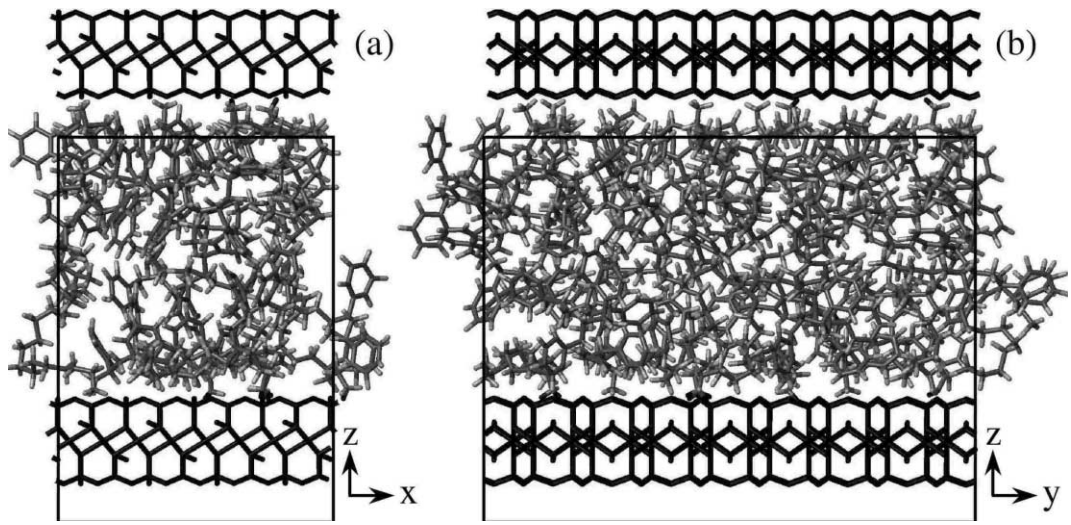


Fig. 2. The two simulation boxes used in this study: with dimensions 2.112 × 1.828 × 3.05 nm (a), and 4.224 × 3.656 × 3.05 nm (b). For all the results discussed herein (density profiles, segmental dynamics, and density/dynamics covariances) there were no differences between the two systems.

[17] and, after subtracting the wall thickness, it allows for a 2.05 nm thin film of organics between the two solid surfaces. The MD runs were carried out in an NVT ensemble [22], where the number of particles ($N$) is chosen based on the experimentally measured material amounts. The grafting density of the surfactant chains (which are octadecyl-ammonium molecules) is well-known and characteristic of the silicate surface [23]. Our grafting density ($\sigma_{\text{graft}} = 1/0.97$ nm$^2$) corresponds to fluorohectorite [23], which is the silicate used in the NMR studies, and dictates 32 (eight for the small box) octadecyl-ammonium cations over the two solid surfaces. Furthermore, from thermogravimetric analysis (TGA), the polymer to surfactant weight ratio can be measured [17], and necessitates for 144 (36 for the smaller box) styrene monomers in the slit. Two systems were extensively studied, the first with styrene chains of 12 monomers each, and the second with chains of 24 monomers (in this case, the small box size is $2.112 \times 3.656 \times 3.05$ nm). Although these chains may be too short to capture the genuine response of long PS macromolecules, they are both longer than the average physisorbed train size of PS in these systems, and also allow for the existence of bridges between the two solid surfaces. Consequently, all the possible segmental dynamics that can develop inside these slit pores can be explored by our MD. Moreover, comparing the two systems with different PS chain lengths does not show any differences *in the segmental dynamics* discussed herein, albeit the substantially longer *chain relaxation times* of the confined 24 monomers compared with the 12 monomers.

One aspect that was scrutinized was the size of the box, especially in connection with the *segmental dynamics correlation lengths* in these systems. Comparison between two systems (a smaller versus a larger, Fig. 2) did not reveal any differences in the segmental dynamics, and in the other results discussed herein (density profiles, correlations of segmental dynamics, and covariance between local density and segmental dynamics); this is why we decided to use the (computationally less intensive) smaller box for the longer times simulated, and compare against shorter runs performed for the larger box. Another more subtle effect of the finite size is the pbc artificial correlations between fast-relaxing moieties that are in close spatial proximity ($\sim 1/2$ box size) across periodic boundary conditions. In our systems, we have checked extensively for such correlations and we found none. The reason is that such fast-relax-

ing elements (e.g. fast-phenyls) are separated by slow-relaxing moieties (e.g. kinetically hindered PS segments), which are effectively immobilized for the duration of each productive MD run. These 'immobile' molecule segments shield against any density or dynamical correlations between species that are on the opposite sides of them.

The force-fields for polystyrene, and its interactions with the alkyl-ammoniums (tabulated in Table 1), are the same as recent PS simulations by Müller-Plathe [24]. The interactions between the silicate and the organic molecules (styrene and aliphatic chains) is based on our earlier simulation work investigating the structure of alkyl-ammonium modified silicates [23]. The silicate partial charges, crystal structure and silicate-cation interactions were developed by Chan and Panagiotopoulos [25], and were proven to reproduce faithfully the hydration behavior of these layered inorganic crystals.

The solid surface atoms were constrained to their equilibrium positions via harmonic springs, which allowed for thermal vibration. The temperature of the surfactant and the polymer was stabilized via a weak coupling to a heat bath by the Berendsen thermostat [26]. Neighbor lists were used for the LJ interactions, and a particle–particle/particle–mesh scheme with Ewald sums for the coulombic interactions. Since the silicate surface is negatively charged (for fluorohectorite — $1q_e/0.97$ nm$^2$), the positive ammoniums have a strong Coulombic attraction to the surfaces; only once, and for the highest temperature studied (470 K), did we observe one of the ammoniums to momentarily desorb from the surface and re-physisorb on a different position on the surface. Thus, for all practical purposes, one can think of the octadecyl-ammoniums as end-tethered on the surfaces.

Probably the most crucial and important aspect of these simulations is the way we selected to sample the configuration phase-space. A simple Configurational Biased Monte Carlo (CBMC) scheme was developed to produce intercalated alkane and alkane surfactant configurations [27]. For the polystyrene systems, however, — where the phenyl sidechains prohibit the use of a simple CBMC approach — a more elaborate route was necessary. The rotational-isomeric-state (RIS) model was used to create initial polymer conformations of PS [28]. Conformations that fit in the interlayer gallery are chosen, and equilibrated by an off-lattice Monte Carlo scheme that employs random displacements of the backbone atoms and Orientational Biased Monte Carlo rotations of the phenyl rings; the surfactants were equilibrated by CBMC attempts in coexistence with the polymer chains. It is critical to have many independent, well-equilibrated initial configurations of the systems to be simulated. As the polymer is held together by strong covalent bonds, the relaxation of the chains is determined by the *slowest* moving segments along the polymer. Even though mobile segments are expected to exist in large numbers [20], they will be bonded to portions of the polymer that remain 'frozen' for timescales vastly longer than what is accessible through MD. Therefore, the only realistic way to explore a large portion of the configurational space is to start with many *independent* initial system conformations and perform productive MD simulations of a few (10–100) ns. Typically, we used ten independent initial configurations for each temperature and we followed each system for 100 ns at $T = 350$ K, 50 ns at $T = 370$ and 390 K, and 10 ns at higher temperatures.

We feel that this computer simulation approach improves our insight in the molecular processes that underlie the striking behavior of the polymer/silicate nanocomposites, and thus can further our molecular level understanding of the nature of polymers in nanometer confinements in general [17]. From this standpoint, we will proceed to describe the behavior of the confined PS systems in a comparative way between simulation and experimental findings.

## 3. Polystyrene in 2 nm thin slit pores

### 3.1. Structure of the confined film

In Fig. 3, the density profiles across the slit pore are shown for different components of the confined organic film. These density profiles correspond to the probability of finding the corre-

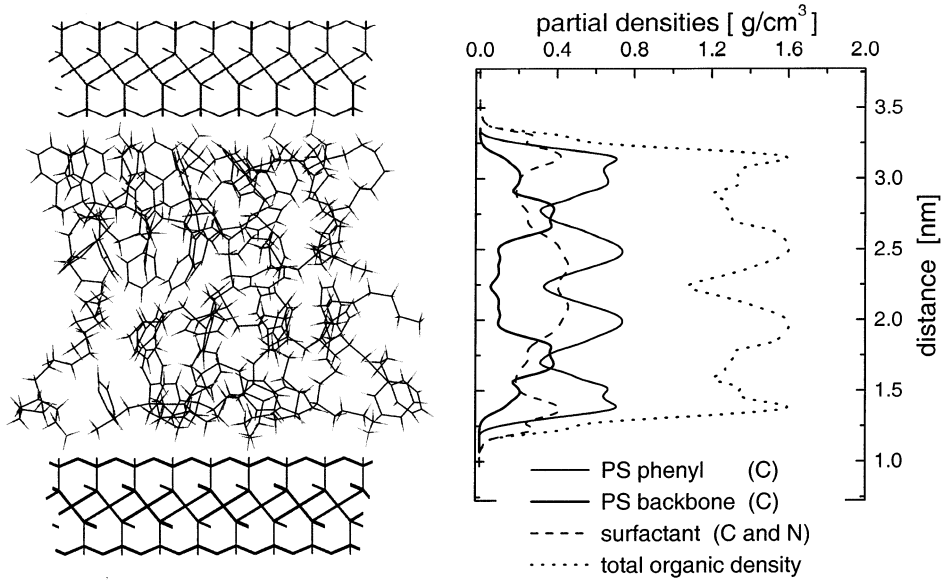


Fig. 3. Density profiles versus distance normal to the confining surfaces. Partial densities across the slit pore are shown, corresponding to the surfactant carbons and nitrogens (dashed line), the styrene phenyl carbons (light continuous line), styrene methyl, methylene and methine carbons (heavy continuous line), and the total organic density (dotted line).

sponding moieties at a certain distance away from the confining solid surfaces, and are calculated through NVT ensemble averages of productive MD runs starting from *distinctly different* initial system configurations. The usage of several — typically ten — different initial configurations for each simulated temperature is essential, because the relaxation times of both the surfactant molecules and styrene chains reach far beyond the 10–100 ns time periods simulated in each MD run. The same density profiles can also be calculated based solely on the Monte Carlo scheme used to create the initial systems for the MD, and are the same with the MD profiles within the data accuracy. This agreement between the MC and the MD ensembles is an indication that our MD's actually sample a representative portion of phase-space.

From Fig. 3, it is obvious that the mass is distributed across the slit pore in a highly inhomogeneous layered fashion. This kind of layering is seen in all simulations of confined systems, ranging from small molecule simple liquids, to alkane oligomers, to grafted alkanes, to generic Lennard Jones chains and realistic polymers. This layering normal to confining surfaces is attributed to the steric interactions between the walls and the confined fluids, and is macroscopically manifested in SFA experiments by wildly oscillating solvation forces when confined fluids are squeezed between mica surfaces [1–9]. Finally, they are so robust that they remain unaffected even under severe shear flows [11].

What is new about our systems, is that there exist several species across the pore (such as surfactant ammonium and aliphatic groups, as well as aliphatic and aromatic styrene groups) and a preferential layering with respect to the walls is developed. The positively charged ammoniums are found in direct contact with the silicate walls — even at the highest temperatures studied — whereas most of the aliphatic part of the surfactant is preferentially located at the center of the slit (Fig. 3). At the same time, we find that the polymer backbone is predominately located near the confining walls, and at distances of about 0.3–0.7 nm from the solid surface, but more removed, on average, than most of the phenyl sidechains. Often, a short strand of polymer adopts a bridging configuration perpendicular to, and connecting between, both walls. The phenyl rings, which attach

to the backbone at each methine, are similarly found on either side of the backbone, and dominate the organic matter nearest the silicate surface. Finally, while surfactant methylenes are found distributed all across the slit pore, they bunch preferentially in the middle layer. These layered density profiles provide some clues as to the origin of the confined film structure. The polar phenyl groups that interact strongly with the silicate surface are preferentially located closest to the surface, whereas the aliphatic groups are displaced towards the center of the pore. Obviously, due to the covalent bonds between the styrene phenyls and methines, the backbone cannot be displaced completely in the center of the pore. Similarly, as the head group of the surfactant is tethered via an ionic interaction to the negatively charged silicate, the surfactant cannot be completely displaced from the surface either. As a result, only its aliphatic tails are displaced by the PS in the center of the slit (Fig. 3).

At first glance, all this detail may seem too theoretical. However, the surface sensitive $^{1}H$-$^{29}Si$ cross-polarization NMR does provide a direct check of the validity of this layered structure (Fig. 4 in [20]). This NMR approach does support the above structural description, and finds the styrene segments — phenyls and backbones — close to the surfaces and the surfactant tails removed towards the center of the slit [20]. Moreover, NMR spectroscopy provides insight on the segmental dynamics of the various moieties in the slit pore, as discussed in the next paragraph.

### 3.2. Segmental dynamics of PS in 2 nm slit pores

A combination of surface sensitive $^{1}H$-$^{29}Si$ cross-polarization NMR and quadrupolar echo $^{2}H$ NMR was used to study the segmental dynamics of selectively deuterated PS in 2 nm slit pores [20]. From these recent NMR studies a new and quite unexpected picture is emerging for the dynamics of nanoscopically confined polymers, which was further confirmed by dielectric spectroscopy investigations on a polysiloxane system [19]. Namely, a coexistence of fast and slow segmental dynamics is observed over a wide range of temperatures, below and above the bulk $T_g$ [20]. This very wide distribution of segmental dynamics spanned relaxation times that ranged from much faster to much slower than the ones observed in the bulk, and this behavior was recorded for all the temperatures studied. In other words, very fast motions were observed in the confined polymer for temperatures deep below the bulk $T_g$, where the corresponding bulk polymer was essentially in a solid-like, immobilized, glassy state (Fig. 4); while for temperatures above the bulk $T_g$, there still exist many segments that remain solid-like and immobilized in the confined systems [20], when at the same temperatures the bulk PS is in a molten, liquid-like state.

Our molecular modeling approach is a conscientious effort to unveil the atomic scale origins of these dynamical inhomogeneities. To this end, we simulated the system depicted in Fig. 1 for several temperatures in the same $T$-range of the $^{2}H$ NMR experiments. We monitor segmental mobility

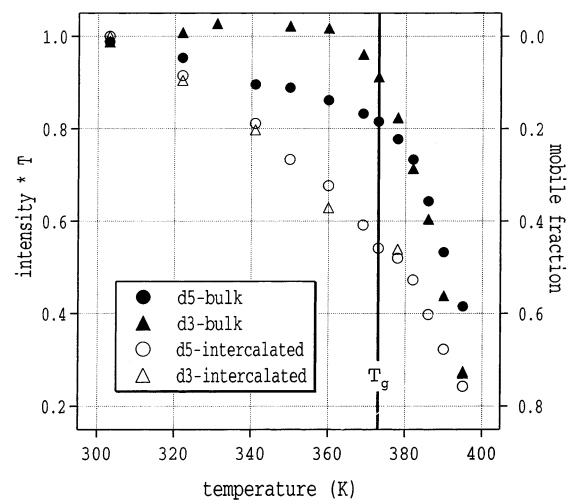


Fig. 4. Quadrupolar-echo $^{2}H$ NMR intensities multiplied by $T$, which corrects for the Curie temperature decrease of observable intensity with increased $T$. Data are shown for selectively deuterated PS (at the backbone and at the phenyl rings, d-3 and d-5 PS, respectively), in bulk and intercalated in organically-modified FH. Intensities less than one correspond to $^{2}H$ sites mobile on the time scale of the spin echo experiment, as is indicated in the right-hand axis. In bulk, ring modes are enabled somewhat below $T_g$, while backbone modes become significant only near $T_g$. In intercalated samples, the two modes are coupled and grow in over a broad temperature range from well below $T_g$, suggesting the existence of faster modes in confined PS than are found in bulk PS (from [20]).

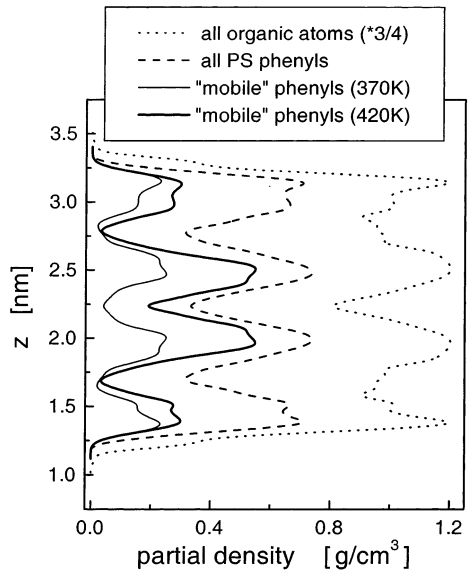


Fig. 5. Density profiles versus distance for all the phenyl carbons (dashed line) and the carbons belonging to mobile phenyls (at 370 K light line, and 420 K heavy line). With ascending temperature the number of mobile phenyls increases, as can be enumerated by the area under the corresponding profiles, and at the same time, the mobile phenyls are preferentially located in the center of the slit. The total organic density is also shown (dotted line) scaled by 0.75.

much like the NMR is doing, by following the relaxation of the C–H bond reorientation. Beyond translation, one can define two types of phenyl reorientations: the 'flipping' around the phenyl axis, and the 'rocking' of this axis. For the backbone methylenes and methines, C–H reorientation takes place by trans-to-gauche isomerization. For NMR, 'mobile' are those C–H bonds that are characterized by relaxation times smaller than the NMR echo spacing ($\tau = 20$ μs). In our simulations, we define as mobile those phenyls that are characterized by relaxation times shorter than $\tau$, as measured from the time autocorrelation function of the corresponding C–H bond vectors [21]. For both segmental moieties, we found an increasing number of mobile entities across the slit with ascending temperature.

Focusing on the phenyl ring dynamics, we show in Fig. 5 the partial densities of the carbons belonging to 'mobile' phenyl rings, for two different temperatures (370 and 420 K). In Fig. 6(a), we quantify the percentage of mobile phenyls as a function of temperature. From these two figures, it becomes obvious that with increasing temperature the number of mobile phenyls increases, and also these mobile rings are located increasingly in the center of the pore. This is not unexpected as it was observed in the NMR experiments. Since the mobile phenyls are located both in the center of the slit pore, as well as near the surfaces — albeit in smaller numbers — the fast segmental dynamics do not seem to originate from the location of the segments across the pore. Motivated from MD simulations in glass forming simple liquids [29], we can check the correlation between the segmental dynamics and the *local* structure inside

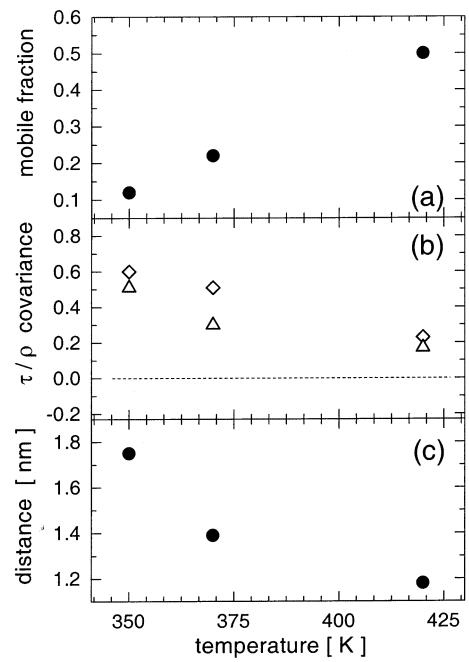


Fig. 6. Some aspects of the mobile phenyl rings as a function of temperature: (a) the mobile fraction of phenyls, characterized by fast orientational relaxations through ring 'flips' and/or axis 'rocking'. (b) The covariance of the relaxation time and the local density for the mobile phenyls, the positive covariance denotes that fast relaxing phenyls are located in lower-than-average local density regions (◇ flipping, △ rocking). (c) The average distance between mobile phenyls in the confined system, the decrease with $T$ is due to the increased number of mobile phenyls, and also their tendency to preferential concentrate in the middle of the slit pore bunched in groups at higher temperatures.

the confined film. This can be realized through the estimation of the covariance of the segmental relaxation and the local density, defined as:

$$\mathrm{cov}(\tau,\rho) \equiv \frac{\langle(\tau - \langle\tau\rangle)\cdot(\rho - \langle\rho\rangle)\rangle}{\sqrt{\sigma^2(\tau)\sigma^2(\rho)}} \quad (1)$$

where, $\tau$ is the segmental relaxation time of a particular phenyl, $\langle\tau\rangle$ is the ensemble average over all phenyls, $\langle\rho\rangle$ is the average density across the slit pore, and $\rho$ is the local density around the phenyl in question. $\sigma^2(\tau)$ and $\sigma^2(\rho)$ are the ensemble variances of the relaxation times and density, respectively. Following this definition, maximum correlation between fast segmental relaxations and low local densities (or equivalently slow segmental relaxations and high local densities) yields a value of $\mathrm{cov}(\tau,\rho) = +1$. Or, for the mobile phenyls of Fig. 6(a):

$$\mathrm{cov} = \begin{cases} +1 & \text{all fast segmental dynamics at local density minima} \\ 0 & \text{nocorrelation between segmental dynamics and local density} \\ -1 & \text{all fast segmental dynamics at local density maxima} \end{cases} \quad (2)$$

The relaxation time/local structure covariance for the mobile phenyls is shown in Fig. 6(b). For the lower temperatures simulated there exists a strong correlation between the local structure and the segmental relaxation. Namely, the fast relaxing phenyls are located in regions where the local density is low (independent of whether they are close to the walls, or in the center of the slit; and independent of whether the C–H relaxation takes place through 'flipping' or 'rocking' motions). As the temperature increases this correlation seems to decay in magnitude, although it still remains positive.

In fact, as the temperature increases, the number of mobile phenyls also increases in such a degree that large volumes in the middle part of the slit consist solely of phenyls with fast segmental dynamics. This reflects in a decreasing average distance between fast relaxing phenyls (as seen in Fig. 6(c)). Furthermore, careful analysis of the MD trajectories reveals that at the lower temperatures there exist only a few segments with fast dynamics, which are isolated from each-other inside the confined film. As the temperature increases, 'groups' of mobile phenyls are formed, especially in the center of the slit pore (Fig. 7); however, despite their proximity, the motions of the phenyls within the same 'group' are not correlated nor cooperative. For all the temperatures simulated (even above 420 K) there exists a large number of immobilized phenyl rings in the immediate vicinity of the confining surfaces, where the organic film is locally densified by the silicate surfaces. The relaxation of these slow phenyls is markedly temperature independent, at least for the time scales that our MD simulations probe. This is in general agreement with the cross-polarization NMR studies, which suggest that styrene moieties in the center of the slits are more mobile, while chain elements (phenyls, methylenes, and methines) interacting with the surface are dynamically inhibited.

Similar analysis for the backbone segmental dynamics reveals the same trends as discussed above for the phenyls [21]. That is, fast backbone segmental dynamics are predominately found in regions where the local density is low, and with increasing temperature mostly in the center of the slit pore. Furthermore, an interesting observation is that the fastest relaxing phenyls are covalently bonded to the fastest backbone segments, and the same for the slowest moving backbones and phenyls. This was not obvious, or intuitively expected, as the phenyl segmental relaxation (e.g. through flipping) does not require backbone reorientation. For example, in bulk — unconfined — PS chains phenyl modes are enabled at temperatures below $T_g$ where the backbone remains rigid; backbone modes start only near $T_g$. Although a more detailed analysis is necessary, this connectivity between moieties with fast segmental relaxations could be the reason that the phenyl and the backbone dynamics are strongly coupled in the confined films (Fig. 4).

Due to the existence of a large number of alkyl-ammonium molecules in our confined sys-

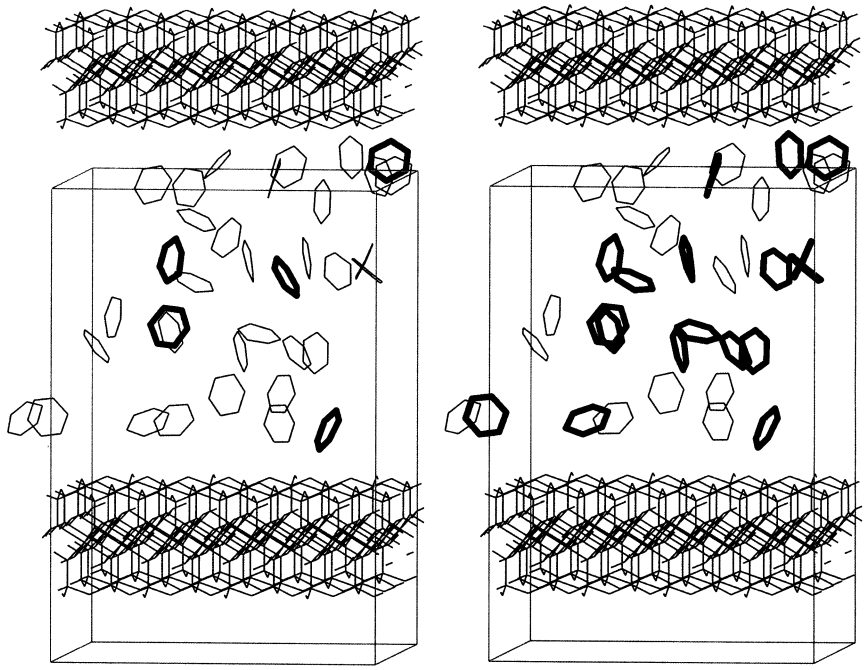

Fig. 7. All the PS phenyls are shown and the ones with fast segmental dynamics are highlighted. The hydrogen atoms, the polymer backbones, and the surfactant molecules are omitted for clarity. To promote comparison, the same system configuration at two different temperatures is shown (left: 350 K, right: 420 K). For the lower temperature the mobile phenyls are isolated, and are located in parts of the system where the local density is low. At 420 K, regions of closely bunched phenyls with fast segmental dynamics develop, especially in the center of the slit, but there also still exist isolated mobile phenyls especially in the low local density regions near the confining surfaces.

tems, that can 'plasticize' the polymer, it was not initially clear [20] whether these dynamical inhomogeneities arise from plasticization effects, or whether are confinement induced. On this point, our simulations show that the fast segmental relaxations are not correlated to the surfactant proximity and/or dynamics [21], but originate from the confinement-induced density inhomogeneities. This is further supported by other experimental studies of different systems, which also provide strong indications that these segmental dynamical are associated with the polymer confinement, (*i*) $^2$H NMR lineshape studies by Zax and coworkers, also observed coexisting fast and slow modes in poly(ethylene oxide), which was intercalated in the same silicate as the PS herein, but in absence of any surfactant whatsoever [30,31]. In this case, despite the much narrower confinements (0.8 nm), the intercalated PEO chains exhibit substantial segmental motion [30,31]. (*ii*) Dielectric spectroscopy of poly(methyl phenyl siloxanes) (with a $T_g$ more than 150 K below the PS $T_g$) report a similar coexistence of ultra-fast and solid-like (slow) relaxations over a wide range of temperatures [19], and measure an extraordinarily fast relaxation, which is completely absent in the bulk unconfined polymer.

Finally, we would like to commend on the quantitative comparison between the molecular simulations and the NMR experiments. The assiduous reader must have noticed that the simulation enumeration of the mobile fraction (Fig. 6(a)) underestimates the NMR measured one (Fig. 4), albeit capturing the correct temperature dependence. This discrepancy can result from several sources, such as the uncertainties in the relaxation time calculation, and phenomena that become important after the 100 ns probed by our MD runs (such as polymer diffusion or desorption). However, none of these two reasons can adequately account for the deviation between the experimental

and simulation values. We believe that the cause of this difference lies in the styrene and alkyl-ammonium densities used in our simulations, which must be higher than the ones in the intercalated experimental systems. Even though we based our densities on the TGA estimated quantities, the gravimetric method may also measure polymers physisorbed on the outside of the silicate stacks, i.e. not in the confined film. Since there exists a very strong dependence between the density and the fast segmental dynamics, minute deviations in density can result in large variations in the system dynamics. Nevertheless, the aim of the simulations is not to quantitatively reproduce the experimental observations, but to reveal the origins of the experimentally observed behavior, and provide insight to the relevant molecular processes.

### *3.3. The glass transition in 2 nm confinements*

The glass transition in thin (10–150 nm) supported polystyrene films has been extensively studied by several methods, including ellipsometry, X-ray reflectivity, positron annihilation lifetime spectroscopy (PALS), and Brillouin light scattering [32–37]. Although many of the findings still remain controversial, some consensus has been reached [38]. Specifically, it is believed that where there exist strong specific interactions between the polymer and the surface, the glass transition temperature ($T_g$) increases, whereas near weak interacting $SiO_x$ surfaces $T_g$ decreases. In efforts to explain these results some studies [37] propose the existence of a 50 nm immobilized, rigid, 'dead' layer of polymer adsorbed on the solid surfaces, in where no $T_g$ is observed and the polymer and segmental dynamics are believed to be inhibited.

Our intercalated polymers offer a great model system to study the glass transition in a much more severe confinement of 2 nm, where *all* the polymer segments are adsorbed on the confining surfaces. These systems provide the means to directly explore the behavior of the adsorbed polymers, without the existence of any non-adsorbed — bulk — material. In Fig. 4 any evidence of a glass transition is completely absent in the confined polymer systems, whereas is clearly observed in the corresponding bulk. In order to further explore this response, we used DSC to study the same intercalated material used in the NMR, and no glass transition was detected in the confined systems (Fig. 8). Considering both the NMR and the DSC data, it becomes obvious that there seems to be no clear glass transition in these ultra-confined polymers inside the 2 nm slit pores. This is in concert with extensive studies investigating the glass transition of poly(ethylene oxide) intercalated in similar slit pores, employing DSC and thermally stimulated dielectric depolarization [39].

If we briefly consider the theoretical descriptions of the glass transition, we find that many modern approaches emphasize the existence of a 'cooperativity volume' that increases in size as $T$ approaches $T_g$. This volume consists of moieties with cooperatively rearranging segmental dynamics, and characteristic space dimensions of about 4 nm or larger. Apparently, both simulations and experiments suggest that in our 2 nm slit pores the creation of such cooperativity regions is strongly

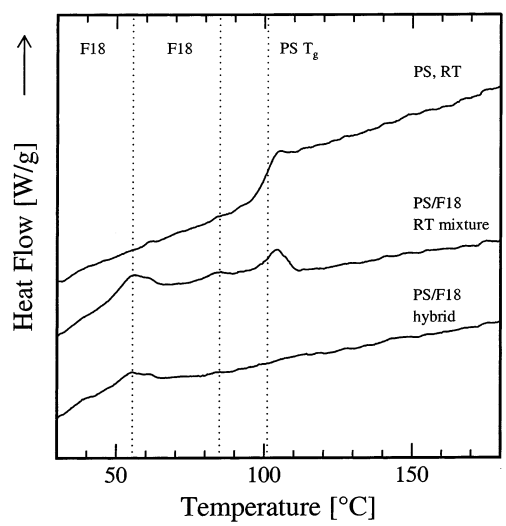


Fig. 8. Differential scanning calorimetry study of bulk polystyrene, PS/octadecyl-ammonium FH (F18) physically mixed at room temperature (RT), and PS intercalated in F18 (the same system used in the NMR studies). Although in the neat polymer and the polymer/silicate mixture the glass transition is evident, it seems to be suppressed when the same polymer is confined in 2 nm slit pores (figure adopted from [17]).

perturbed by the severe confinement size. This raises the issue whether in these slit pore geometries bulk-scale cooperative relaxations — traditionally associated with the glass transition — are even possible. However, the assumption that the adsorbed polymer segments create a rigid, 'dead' layer seems to be at odds with our simulation findings discussed in the earlier paragraph. On the contrary, we find the adsorbed polymer segments to have a very rich dynamical behavior that simultaneously includes ultra-fast and solid-like slow relaxations.

## 4. Conclusions

Complementary NMR experiments and MD molecular modeling approaches are employed to explore polystyrene molecules confined in 2 nm slit pores, defined by alkyl-ammonium modified layered-silicate surfaces.

The simulations suggest that the confined film adopts a layered structure normal to the solid surfaces, with the polar phenyls dominating the organic material adsorbed on the walls, and the aliphatic groups predominately in the center of the pore. This layered structure, with the polar styrene groups preferentially on the surfaces, reflects on $^{1}H$-$^{29}Si$ cross-polarization NMR measurements.

NMR reveals a coexistence of ultra-fast and solid-like slow segmental dynamics throughout a wide temperature range, below and above $T_g$, for both the styrene phenyl and the backbone groups. The mobile moieties concentrate at the center of the slit pore, especially for the higher temperatures. The molecular simulations attribute these dynamical inhomogeneities to confinement-induced density inhomogeneities. Namely, the moieties with fast segmental dynamics are located in local density minima. Moreover, they show that at low temperatures the fast moving species are isolated throughout the confined film, whereas with increasing temperature, the mobile moieties increase in number and bunch up in groups especially in the middle of the pore.

Finally, NMR suggests, and DSC confirms, that there is no detectable glass transition inside the 2 nm confined polymer. This leads us to the conclusion that such severe confinements hinder the creation of extended regions with cooperative segmental dynamics, which underlie the glass transition.

## Acknowledgements

This work was supported by a Wilson Research Initiation grant from the EMS College at Penn State. We would like to thank Dr R. Vaia for insightful discussions and for providing the DSC data in Fig. 8.

## References

[1] H.K. Christenson, J. Chem. Phys. 78 (1983) 6906.
[2] D.Y.C. Chan, R.G. Horn, J. Chem. Phys. 83 (1985) 5311.
[3] J.P. Montfort, G. Hadziioannou, J. Chem. Phys. 88 (1988) 7187.
[4] M.L. Gee, et al., J. Chem. Phys. 93 (1990) 1895.
[5] J. van Alsten, S. Granick, Macromolecules 23 (1990) 4856.
[6] S. Granick, Science 253 (1991) 1374.
[7] H. Hu, G.A. Carson, S. Granick, Phys. Rev. Lett. 66 (1991) 2758.
[8] J. Klein, E. Kumacheva, Science 269 (1995) 816.
[9] J. Israelachvili, Intermolecular and Surface Forces, Academic Press, 1991.
[10] I. Bitsanis, C. Pan, J. Chem. Phys. 99 (1993) 5520.
[11] E. Manias, G. Hadziioannou, G. ten Brinke, Langmuir 12 (1996) 4587.
[12] E. Manias, G. Hadziioannou, I. Bitsanis, G. ten Brinke, Europhys. Lett. 24 (1993) 99.
[13] E. Manias, I. Bitsanis, G. Hadziioannou, G. ten Brinke, Europhys. Lett. 33 (1996) 371.
[14] D. Tabor, R.H. Winterton, Proc. R. Soc. London A312 (1969) 543.
[15] D. Tabor, J.N. Israelachvilli, Proc. R. Soc. London A331 (1972) 19.
[16] J.N. Israelachvilli, G.E. Adams, J. Chem. Soc. Faraday Trans. I 74 (1978) 975.
[17] E. Giannelis, R. Krishnamoorti, E. Manias, Adv. Polymer Sci. 138 (1998) 107.
[18] M. Alexandre, P. Dubois, Mat. Sci. Eng. R: Reports 28 (2000) 1.
[19] S. Anastasiadis, K. Karatasos, G. Vlachos, E. Giannelis, E. Manias, Phys. Rev. Lett. 84 (2000) 915.
[20] D. Zax, D.K. Yang, R. Santos, H. Hegemann, E. Giannelis, E. Manias, J. Chem. Phys. 112 (2000) 2945.
[21] V. Kuppa, E. Manias, ACS Symp. Ser., in press (2001).

[22] During the NVT ensemble simulations we have also followed the pressure of the systems (through the stress tensor at the walls). The pressure is maintained constant for each temperature, and there exists a slight only change (less than a few percent) across different temperatures. Thus, this NVT ensemble could also be considered as a collection of microstates from an isobaric (NPT) ensemble with a *weak coupling* to a pressure [26].
[23] E. Hackett, E. Manias, E.P. Giannelis, J. Chem. Phys. 108 (1998) 7410.
[24] F. Müller-Plathe, Macromolecules 29 (1996) 4782 complete information on the PS force-field can be obtained from Müller-Plathe's web site at the Max-Planck Inst.
[25] Y. Chan, Computer Simulations of 2:1 Silicates Hydration, Master Thesis (under A.Z. Panagiotopoulos), Cornell University, 1997.
[26] H.J.C. Berendsen, J.P.M. Postma, W.F. van Gunsteren, A.D. Nola, J.R. Haak, J. Chem. Phys. 81 (1984) 3684.
[27] E. Hackett, E.P. Giannelis, E. Manias, J. Chem. Phys., in press (2001).
[28] W.L. Mattice, U.W. Suter, Conformational Theory of Large Molecules: The Rotational Isomeric State Model in Macromolecular Systems, Wiley, New York, 1994.
[29] J. Qian, R. Hentschke, A. Heuer, J. Chem. Phys. 111 (1999) 10177.
[30] S. Wong, S. Vasudevan, R. Vaia, E. Giannelis, D. Zax, J. Am. Chem. Soc. 117 (1995) 7568.
[31] S. Wong, R. Vaia, E. Giannelis, D. Zax, Solid State Ionics 86 (1996) 547.
[32] J. Keddie, R. Jones, R. Cory, Europhys. Lett. 27 (1994) 59.
[33] J. Keddie, R. Jones, J. Isr. Chem. Soc. 35 (1995) 21.
[34] J. Forrest, K. Danloki-Veress, J. Dutcher, Phys. Rev. E 56 (1997) 5705.
[35] W. Wallace, J. van Zanten, W. Wu, Phys. Rev. E 52 (1994) R3329.
[36] W. Wallace, J. van Zanten, W. Wu, Phys. Rev. E 53 (1996) R2053.
[37] G.B. DeMaggio, W.E. Frieze, D.W. Gidley, M. Zhu, H.A. Hristov, A.F. Yee, Phys. Rev. Lett. 78 (1997) 1524.
[38] J. Forrest, R. Jones, in: A. Karim, S. Kumar (Eds.), Polymer Surfaces, Interfaces and Thin Films, World Scientific, 2000, p. 251.
[39] R. Vaia, B. Sauer, O. Tse, E. Giannelis, J. Polymer Sci. Part B: Polymer Phys. 35 (1997) 59.